PART IV

STUDIES ON STRATUM CORNEUM LIPIDS FROM OTHER SKIN SOURCES SHOWING A BARRIER DYSFUNCTION

CHAPTER 9

SKIN BARRIER LIPID COMPOSITION AND ORGANIZATION IN NETHERTON SYNDROME PATIENTS

J. van Smeden[1,*], M. Janssens[1,*], W.A. Boiten[1], R.J. Vreeken[2], A. Hovnanian[3], J.A. Bouwstra[1]

[1] Division of Drug Delivery Technology, Leiden Academic Centre for Drug Research, Leiden University, Leiden, The Netherlands.
[2] Netherlands Metabolomics Centre, Leiden Academic Centre for Drug Research, Leiden University, Leiden, The Netherlands.
[3] Pathology Department and MAGEC Center for Rare Cutaneous Diseases, Hopital Necker-Enfants Malades, APHP, Paris, France.
*Both authors contributed equally to this work

Submitted

Abstract

Netherton Syndrome (NTS) is a rare genetic skin disease that is characterized by erythroderma, hair shaft defects, and severe atopic manifestations. The disease is caused by mutations in the serine protease inhibitor Kazal-type 5 (SPINK5) gene, which encodes the protease inhibitor lympho-epithelial Kazal-type–related inhibitor (LEKTI). Lack of LEKTI causes epidermal proteases hyperactivity, which results in stratum corneum (SC) detachment. NTS patients have an impaired skin barrier function. Besides barrier proteins, SC lipids are also crucial for the skin barrier. The lipids primarily consist of ceramides (CERs), free fatty acids (FFAs) and cholesterol. To date, hardly any information is available on the SC lipid composition and organization in SC of patients with NTS. Therefore, the aim of the present study is to determine the SC lipid composition and organization in NTS patients.

We investigated the SC lipids by means of mass spectrometry, infrared spectroscopy and X-ray diffraction. We studied the lipid subclasses as well as the chain length distributions. A decreased FFA chain length and an increased level of monounsaturated FFAs was observed in SC of NTS patients compared to controls. Furthermore, the level of short-chain CERs was increased in NTS patients, and in a subgroup of patients we observed a strong reduction in long-chain CER levels. The changes in lipid composition modified the lipid organization: an increased disordering of the lipids compared to the controls. This study shows that there are striking changes in the lipid composition in NTS that may contribute to the skin barrier dysfunction in NTS.

Introduction

Netherton syndrome (NTS) is a rare skin disorder with an occurrence of 1-3 in 200.000 births and a fatality rate of around 20% in the first year of life by hypernatremic dehydration, electrolyte imbalances, perturbed thermoregulation, failure to thrive, and recurrent infections[1-5]. NTS is characterized by erythroderma, hair shaft defects (bamboo hair), and severe atopic manifestations[6]. In addition, NTS patients show a drastically reduced skin barrier function[7-9]. The skin barrier is primarily located in the outermost layer of the skin, the stratum corneum (SC). The SC consists of flattened corneocytes embedded in a highly ordered lipid matrix. The organization and composition of this lipid matrix seems crucial for the barrier function of the skin, but hardly any information is available on the SC lipids regarding NTS patients. The aim of the present study is therefore to unravel the composition and organization of this SC lipid matrix in NTS.

SC lipids mainly consist of ceramides (CERs), cholesterol (CHOL) and free fatty acids (FFAs). To date, 12 CER subclasses with a wide variation in chain length distribution have been identified in human SC[10,11]. FFAs mainly consist of saturated carbon-chains with lengths varying between 16 and 36 carbon atoms, of which the most abundant chain lengths are 24 and 26 carbon atoms[12,13]. In healthy SC, lipids form two lamellar phases with repeat distances of approximately 6 and 13 nm referred to as the short periodicity phase (SPP) and long periodicity phase (LPP), respectively[14,15]. Within the lamellae, the lipids form a dense (orthorhombic, highly ordered lipid chains) lateral organization, although lipid domains with a less dense (hexagonal, less ordered lipid chains) lipid organization also co-exist. Both the lipid composition and lipid organization are crucial for a proper SC barrier function. Recent studies show the important role of the SC lipids in the skin barrier function of atopic eczema (AE) patients[16,17], a skin disease often linked to NTS because of its shared symptoms[18,19]. We demonstrated a modified chain length distribution in CERs in SC of AE patients. This change resulted in an altered SC lipid organization, which in turn was correlated with an impaired skin barrier function.

NTS is caused by mutations in the serine protease inhibitor Kazal-type 5 (SPINK5) gene. These mutations result in loss of function of lympho-epithelial Kazal-type–related inhibitor (LEKTI)[20]. LEKTI is described in relation to proteins involved in proliferation and differentiation of keratinocytes. In addition, several LEKTI-domains can efficiently inhibit the enzyme activity of various subtypes of kallikreins (KLKs): KLK5, KLK7 and KLK14. Lack of active LEKTI domains lead to increased activity of these KLKs, thereby affecting various biological processes that will have a detrimental effect on the skin barrier:

i) KLKs 5 and 7 are involved in the desquamation process, that is, the degradation of the corneodesmosomes linking the corneocytes in the SC[21-26]. Reduction in the activity

of LEKTI, which inhibits the activity of these enzymes, causes epidermal proteases hyperactivity resulting in SC detachment[27].

ii) KLKs 5 and 14 induce cutaneous inflammation through proteinase-activated receptor 2 (PAR2) and NF-κB pathway activation *in vitro*[28], leading to up-regulation of pro-Th2 cytokine thymic stromal lymphopoietin (TSLP), IL1-α, IL8, and TNF-α[8,23,29,30]. The production of these cytokines can in turn affect the SC lipid synthesis and thereby the skin barrier[31,32]. Besides, PAR2 activation can lead to abnormal lamellar body secretion that also results in disrupted lipid lamellae and a reduced skin barrier function[7].

iii) KLKs act as catalysts for the proteolysis of the enzymes β-glucocerebrosidase and acid sphingomyelinase[33]. Both enzymes are involved in synthesis of CERs that play an important role in the barrier function of the SC.

iv) Increased activity of KLK5 (as a result of decreased inhibition by LEKTI) leads to hyperactivity of the epidermal protease elastase 2 (ELA2). This results in abnormal processing of filaggrin, a keratin filament-associated protein highly associated with atopic eczema[34]. Filaggrin breakdown products, the natural moisturizing factor (NMF), are suggested to be important for maintaining the acidic nature of the SC: An increase in pH induces premature degradation of corneodesmosomes leading to a disrupted barrier and cohesion of the skin[35]. In addition, an increase in pH can lead to altered catalytic activities of lipid processing enzymes that require an acidic pH for their optimal catalytic activity[36]. Besides these effects of KLKs on the different aspects of the metabolic pathways, KLKs may activate each other or induce self-activation, thereby exacerbating the effects[30,37,38]. NTS patients show different expression of proteins like loricrin, involucrin and the transglutaminases. This disturbs the assembly of the cornified envelope surrounding the corneocytes and may also reduce the SC barrier function[39-41]. Altogether, this results in a drastically reduced barrier function in patients with NTS as measured by transepidermal water loss (TEWL)[7-9].

To date, little is known about the SC lipid composition in NTS. A study of Bonnart *et al*.[34] with transgenic mice overexpressing ELA2 as a model for NTS reported a threefold increase in TEWL, demonstrating a decreased skin barrier function. For the first time, the lipids in total epidermis were analyzed. They observed an increased level of total glucosylceramides and a reduction of sphingomyelin, as well as significant decrease in FFA levels. In addition, it was reported that the lipids form irregular loose stacks of lamellae[7,34,42]. However, no data were reported on individual CER and FFA subclasses and chain length distributions of the lipids. In addition, no quantitative information about the lamellar phases was provided and no information is available on the lateral packing. Therefore, the aim of this study was to perform an in depth analysis of the lipid

composition and organization in SC of patients with NTS.

Our results show that in SC of NTS patients, there is a strong increase in short chain CERs and FFAs as well as an increase in unsaturated FFAs. Furthermore, the lipid chains are more disordered and the lamellar lipid organization is altered. A subgroup of patients showed no lamellar lipid profile at all, and these patients also had the most drastic changes in their SC lipid composition.

Materials and Methods

Study population

The study was conducted in accordance with the Declaration of Helsinki and was approved by the Ethical Committee of Paris Ile de France. Eight patients with classical features of Netherton syndrome were included in the study. They were from different ethnic backgrounds and their age ranged from 8 to 39 years at the time of the study. Patients included four males and four females. Patients ③ and ④, as well as ⑦ and ⑧ are siblings, respectively. Each patient presented congenital ichthyosiform erythroderma, trichorrhexis invaginata, and eczematous like lesions. Four of them had ichthyosis linearis circumflexa (patients ④, ⑥, ⑦ and ⑧). All patients had elevated immunoglobulin E in the serum. Each patient showed negative LEKTI immunostaining on skin biopsy. SPINK5 mutations leading to premature termination codons were identified in each patient.
For comparison, SC from the epidermis of 5 Caucasian subjects (36.2 ± 12.2 years; 3 males) was analyzed, which was obtained after abdominal- or mammaplasty reduction at the hospital. SC was isolated by trypsin digestion, a procedure that does not affect the lipid organization in SC[43] and is described previously[44].

Lipid classification and nomenclature

FFAs are classified according to their shorthand lipid number designation in which the chain length and degree of unsaturation is denoted[45]. For example, octadecenoic acid (oleic acid) is denoted as C18:1. Ceramides consist of a sphingosine base linked to a fatty acid (acyl) chain. In human SC, both chains can vary in the number of carbon atoms. This results in a wide distribution in total chain length, that is, the total number of carbon atoms in both chains. In addition, both chains can have additional functional groups at specific locations. This results in 12 identified subclasses[10,11] that are classified according to the nomenclature of Motta *et al.*[46]: CER [ADS], [AH], [AP], [AS], [EODS], [EOH], [EOP], [EOS], [NDS], [NH], [NP], and [NS] (Figure 1).

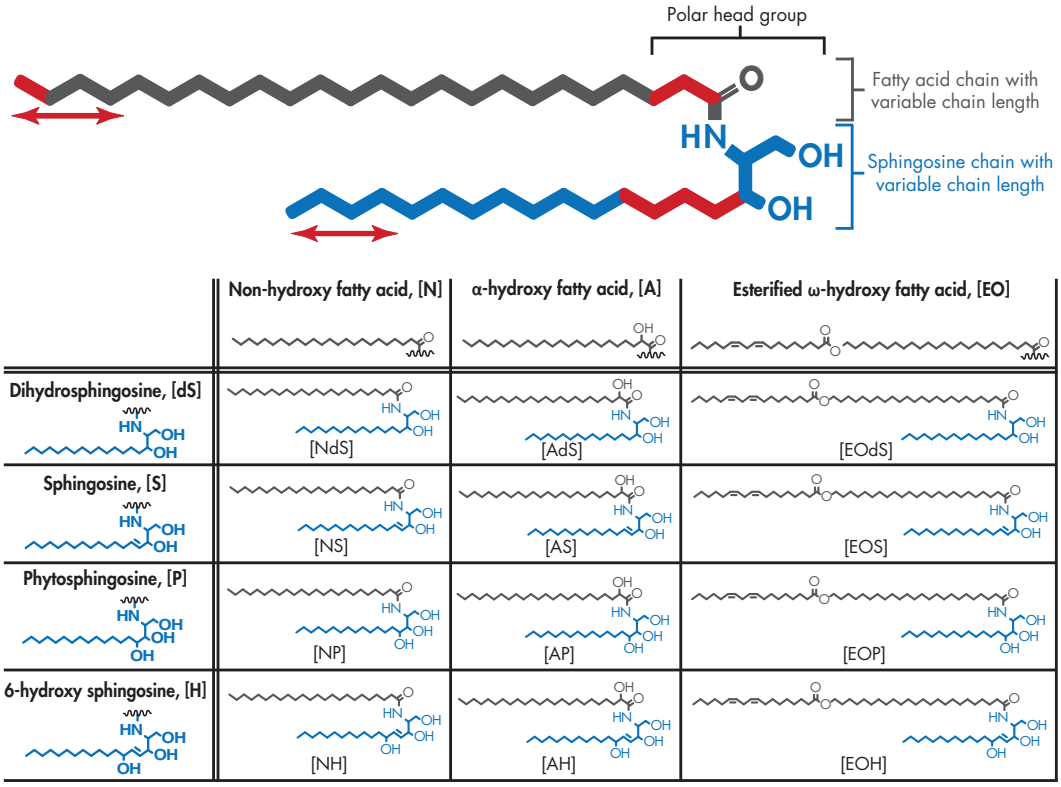

Figure 1: *CER nomenclature and molecular structure. CERs are composed of a sphingoid base (depicted in blue) linked via an amide bond to an acyl chain (gray). Both chains show a variable carbon chains length indicated by the red arrows. This results in a wide distribution of the total CER chain length, i.e. the chain length of the sphingoid base and acyl chain combined. Both chains can have additional functional groups at the carbon positions marked in red. This results in 4 different sphingoid bases (dihydrosphingosine [dS], sphingosine [S], phytosphingosine [P], 6-hydroxy sphingosine [H]) and 3 different acyl chains (non-hydroxy fatty acid [N], α-hydroxy fatty acid [A] and esterified ω-hydroxy fatty acid [EO]). Together, this results in the presence of 12 subclasses denoted as: [NdS], [AdS], [EOdS], [NS], [AS], [EOS], [NP], [AP], [EOP], [NH], [AH], [EOH]. As an example, a CER with a non-hydroxy fatty acid of 16 carbon atoms long and a phytosphingosine base of 18 carbon atoms will be denoted as CER [NP] C34.*

SC lipid extraction and analysis

An enhanced procedure of the commonly used Bligh and Dyer method was performed to extract the lipids from the SC sheets of both NTS patients and control subjects. Afterwards, lipids were analyzed by liquid chromatography coupled to mass spectrometry (LC/MS) to profile the CERs and FFAs. A detailed protocol of the lipid extraction and lipid analysis is described elsewhere[11,47]. Briefly: a three-step sequential extraction procedure of chloroform/methanol/water (1:2:½; 1:1:0 and 2:1:0) was performed to extract all extracellular SC lipids. To enable proper analysis by LC/MS, samples were reconstituted in chloroform/methanol/heptane (2½:2½:95) to obtain a final concentration of 1.0 mg/

mL. Two injections of 10 µl of each lipid sample were performed to analyze sequentially FFAs and CERs, using an Alliance 2695 HPLC system (Waters Milford, MA). The HPLC was coupled to a mass spectrometer (TSQ Quantum, Thermo Finnigan, San Jose, CA) equipped with an APCI ionization source. FFAs were separated using a C18 reverse phase column (Purospher Star LiChroCART, Merck, Darmstadt, Germany) and analyzed in negative ion mode, while separation of CERs was achieved using a normal phase column (PVA-Sil, YMC, Kyoto, Japan) while analyzing in positive ion mode. Xcalibur software version 2.0 was used for data acquisition.

Small angle X-ray diffraction measurements

SC sheets were analyzed by small angle X-ray diffraction (SAXD), performed at the European Synchrotron Radiation Facility (ESRF, Grenoble, France) using station BM26B. SC was hydrated over a 27% NaBr solution during 24h before the measurements. SC sheets were oriented parallel to the primary X-ray beam in order to obtain high quality diffraction patterns. SAXD patterns were detected with a Frelon 2000 charge-couple device (CCD) detector at room temperature for a period of 10 minutes using a microfocus beam, similarly as described elsewhere[48]. The exposure time to the X-rays was kept to a minimum and samples showed no evidence of radiation damage. From the scattering angle, the scattering vector (q) was calculated by $q = 4\pi \sin\theta/\lambda$, in which λ is the wavelength of the X-rays at the sample position and θ the scattering angle. The repeat distance of a lamellar phase can be calculated from the diffraction peaks by $d = n \cdot 2\pi/q_n$, in which n is the order of the peak. This means that a shift in peak position to higher q values results in a shorter repeat distance.

Conformational ordering of the lipids

A high conformational ordering is an indication that the lipids adopt the properties of a crystalline phase, whereas a low conformational ordering indicate that the lipids form a liquid phase. To obtain information on the conformational ordering, Fourier transform infrared (FTIR) spectra were recorded using a Varian 670-IR spectrometer (Varian Inc., Santa Clara, CA) equipped with a broad band liquid nitrogen cooled mercury-cadmium-telluride (MCT) detector and an external sample compartment containing a Gladi*ATR* (Pike, Madison, WI) attenuated total reflection (ATR) accessory with a single reflection diamond. The spectra of patients were collected in attenuated total reflectance (ATR) mode and transmission mode (as a control), and no difference between both methods was observed. SC samples were hydrated over a 27% NaBr solution during 24h. SC was mounted between two ZnSe windows when measured in transmission mode. Samples

were put under a purge of continuous dry air starting 30 minutes before data acquisition. Spectra were acquired as a co-addition of 256 scans at 1 cm^{-1} resolution during 4 minutes. When measuring in ATR mode, 150 spectra were acquired and averaged. The spectral resolution was 2 cm^{-1}. Resolutions Pro 4.1 (Varian Inc.) was used for data acquisition.

Statistical analysis

Statistical analysis was performed using SPSS Statistics. Non-parametric Mann-Whitney tests were performed when comparing 2 groups, unless explicitly noted elsewhere. Differences were considered either weakly significant ($P<0.1$), moderately significant ($P<0.05$), or highly significant ($P<0.005$), and are denoted throughout the manuscript as *, **, and ***, respectively.

Results

Decreased FFA chain length and increased degree of unsaturation in patients with Netherton syndrome

Figure 2 shows data on the FFA composition of NTS patients (red) compared to the control subjects (green). The presence of FFAs <20 carbon atoms, being abundantly present in patients, were not taken into account in the present study as these FFAs are most probably present due to contamination of topical treatments of the NTS patients. It is impossible to distinguish between native FFAs and those from topical formulations. The relative abundance of saturated FFAs and mono-unsaturated FFAs (MUFAs) is shown in Figure 2a. In NTS patients, there is a lower level of saturated FFAs compared to SC of controls (71.3 ± 24.1% and 97.0 ± 1.1%, respectively), and a higher level of MUFAs compared to controls (28.7 ± 24.1% and 3.0 ± 1.1%, respectively). Figure 2b shows the relative chain length distribution of saturated FFAs in NTS patients (red) and in controls (green). The most abundant chain lengths in controls are C24:0 and C26:0. The large standard deviations of the NTS patients are caused by inter-subject variation and not due to methodological variation.

Compared to control subjects, lipids of SC in NTS patients show a shift to shorter FFA chain length: there is a significant increase in FFA C20:0 and C21:0 and a significant decrease in FFAs C24:0, C25:0 and C26:0. Figure 2c shows the chain length distribution of MUFAs. No odd chain length MUFAs were detected in SC from either NTS or control. SC of NTS patients show a significant level of MUFAs C20:1, C22:1, C24:1. On the contrary, control subjects did not show a detectable level of MUFAs ≤C24 (C20:1, C22:1, C24:1) and only very low levels of C26:1, C28:1, C30:1 and >C30:1. From the abundance of both the saturated FFAs and MUFAs, the average chain length for each patient and control was

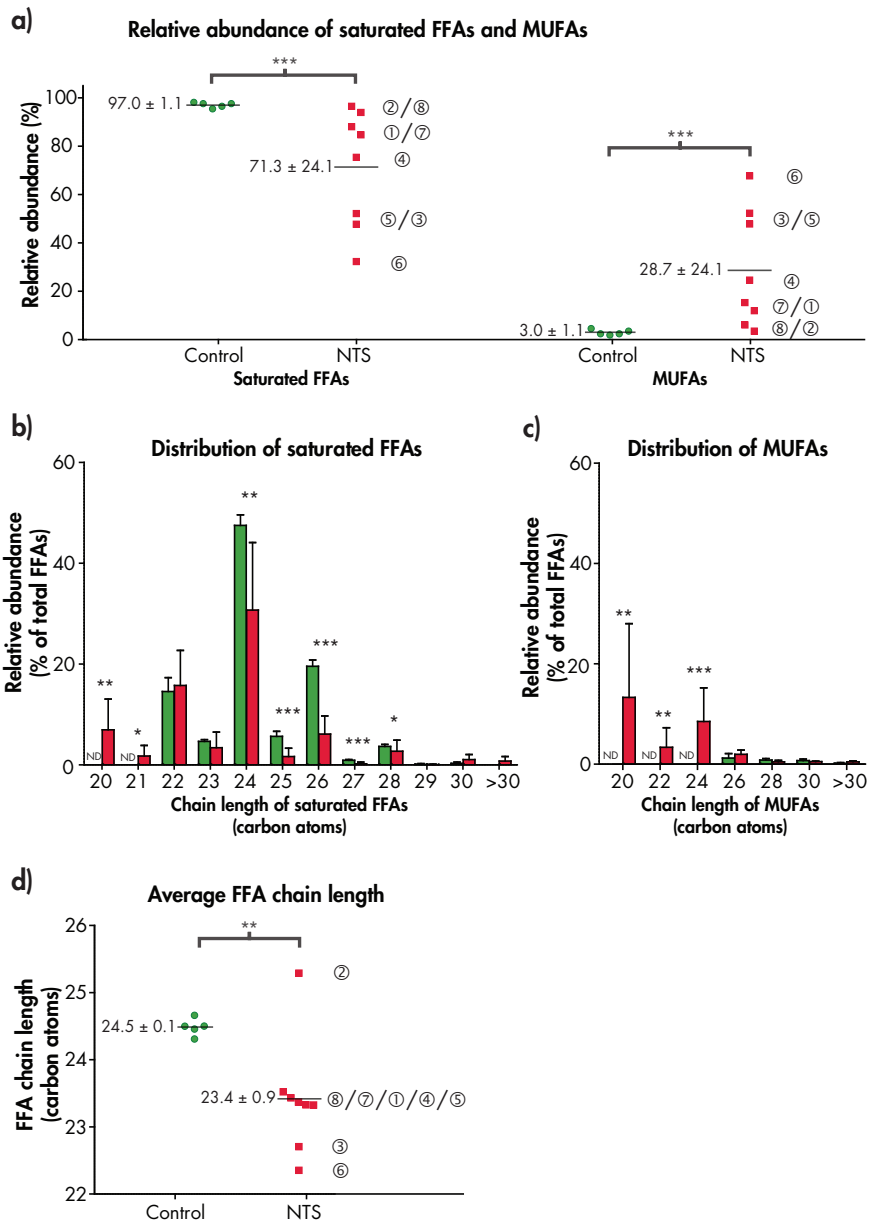

Figure 2: *a) Scatter dot plot showing the relative abundance of saturated FFAs (left) and MUFAs (right).* ***b****) and* ***(c)*** *present bar graphs showing the relative abundance of respectively saturated FFAs and MUFAs. The total abundance of saturated FFAs and MUFAs together was set to 100%.* ***d****) Scatter dot plot showing the average FFA chain length. Controls (n=5) and NTS patients (n=8) are presented as green and red bars/dots, respectively. Error bars represent SD values; Horizontal lines indicate averages. ND means 'not detected'. Individual NTS patients are labeled ①-⑧.*

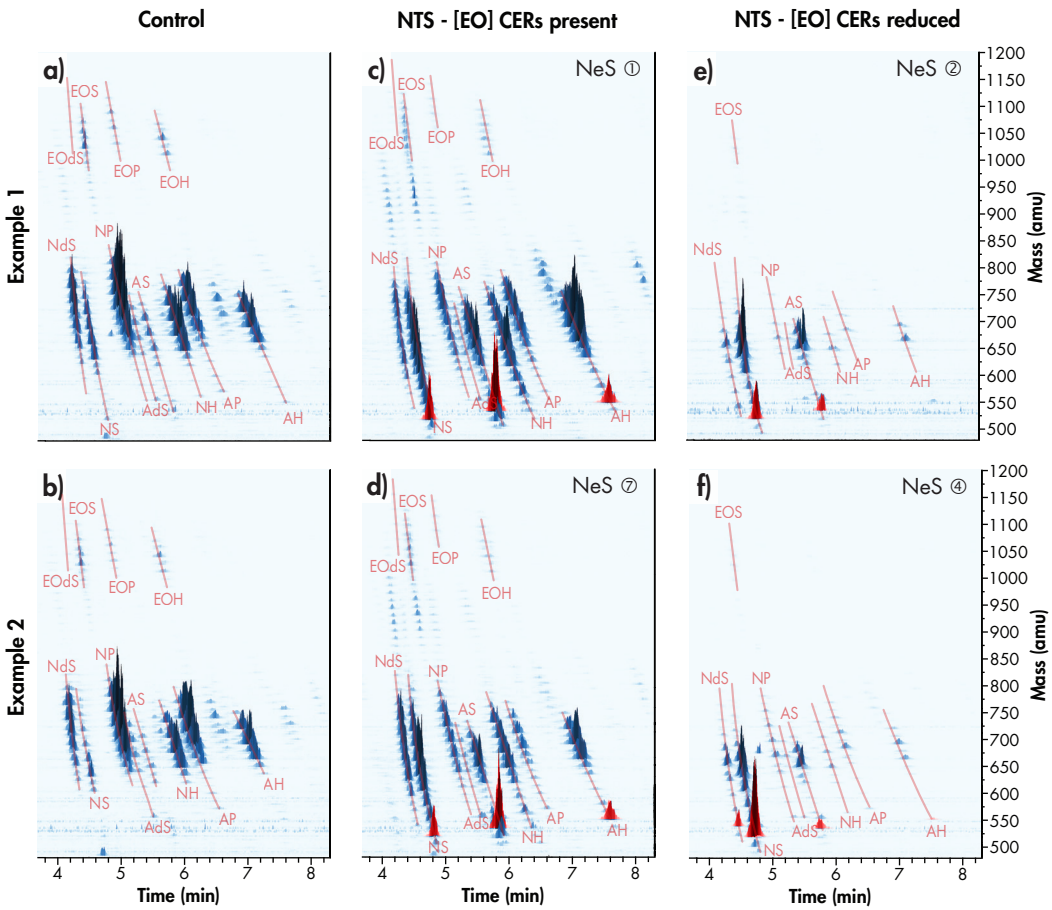

Figure 3: *3D ion chromatograms of control SC (**a** and **b**) and NTS patients (**c**, **d**, **e** and **f**). Retention time (3.6-8.3 min), mass (480-1200 amu), and relative intensity of each peak are shown on the x-, y- and 'z'-axis, respectively. Chromatograms are normalized to their most abundant peak. The chromatograms of the NTS patients show a decreased chain length of the CERs. In addition, in (**e**) and (**f**) there is a decrease in acyl-CERs ([EO] CERs) and a narrower chain length distribution in all other CER subclasses. NTS patients also show an increase in short chain CERs, in particular CERs with a chain length of 34 carbon atoms (C34 CERs), which are indicated in the chromatograms by red peaks. The 3D ion chromatograms of the other controls and NTS patients are listed in Supplementary Figure 1.*

calculated. These results are provided in Figure 2d and show that the average FFA chain length is significantly reduced in NTS patients versus controls (23.4 ± 0.9 and 24.5 ± 0.1 carbon atoms, respectively).

Altered levels of acyl-CERs and short-chain CERs in SC of NTS patients

The CER profiles of 5 controls and 8 NTS patients were studied. The CER profiles of two representative examples of controls and 4 examples of NTS patients are presented in the 3D ion chromatograms in Figure 3. An overview of 3D ion chromatograms of the remaining

NTS patients and control subjects is provided in Supplementary Figure 1. Figures 3a and b show two examples of the CER profiles of control SC. As there was very little difference in the profile of all control subjects, these two pictures closely resemble those of all 5 controls. There are at least 12 CER subclasses depicted, as reported before[11]. Within each CER subclass, a large number of peaks can be observed. Each peak indicates a CER specie with a different chain length: The difference in molecular mass of two sequential CER species within one subgroup is 14 mass units, representing a reduction of one CH_2-group. In all 12 CER subclasses in human SC a wide distribution in their total carbon chain length is observed. The CERs with higher mass values in the upper part of the 3D mass spectrogram belong to the CER [EO] subclasses (also noted as acyl-CERs) and show a chain length distribution between 63-78 carbon atoms. The α-hydroxy [A] and non-hydroxy [N] CER subclasses have shorter chains and therefore lower masses. The carbon chain lengths of these subclasses are between 34-52 and 32-56 carbon atoms, respectively. The 3D ion chromatograms of NTS patients are provided in Figures 3c, d, e and f.

In general, of all CER subclasses, CER [NP] was most significantly reduced, whereas CER subclasses [AS], [NS], and [AH] were least affected. Furthermore, there is a shift in the lipid chain length distribution of NTS patients to lower mass values compared to controls: increased peak intensities in the molecular range between 550 and 650 amu are observed in chromatograms of NTS patients (labeled as red peaks in Figure 3).

The chromatograms of Figures 3c and d are representative for 5 NTS patients (①,⑤,⑥,⑦, and ⑧). In the SC of these patients, all CER subclasses are observed. There is a clear shift to a higher abundance of short-chain CERs. This is particularly the case for CER subclasses [NS], [AS] and [AH], for which a very high peak was observed corresponding to CERs with a very short total carbon chain length of 34 carbon atoms (referred to as C34 CERs). Figures 3e and f show the ion chromatograms representative for the other 3 NTS patients (②,③ and ④). These patients show a clearly distinguishable pattern compared to the other NTS patients: There is a narrow chain length distribution in [A] and [N] subclasses. In addition, the level of acyl-CERs is drastically decreased and the C34 CERs are strongly increased. NTS subject ⑥ also shows a clearly distinguishable pattern in the CER subclasses, but in contrast to the other 3 patients, acyl-CERs were present in this subject (Supplementary Figure 1).

Quantitative results on the relative abundance of acyl-CERs and short-chain CERs are shown in Figures 4a and b, respectively. Control subjects show on average a relative abundance of 8.4 ± 1.9% acyl-CERs. This abundance was comparable for 5 out of 8 NTS patients, but 3 patients show a drastic reduction to ~2.5%. Regarding the abundance of very short chain CERs with a mass lower than 600 amu (corresponding to a total chain

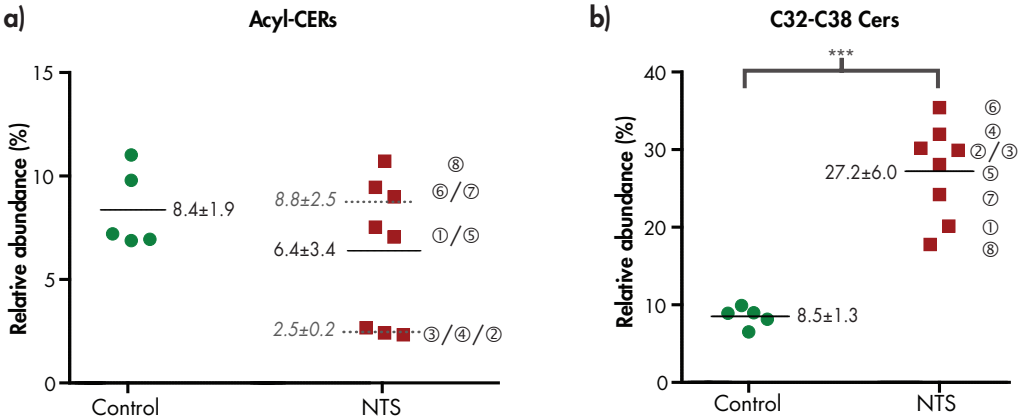

Figure 4: *Dot plots showing the relative abundance of* ***a****) acyl-CERs and* ***b****) short chain CERs (C32-C38). Black horizontal lines and the corresponding values indicate mean values (±SD). Gray dotted lines indicate averages for two different categories observed: 5 NTS patients with normal acyl-CER levels and 3 NTS patients with reduced acyl-CER levels. Individual NTS patients are labeled ①-⑧.*

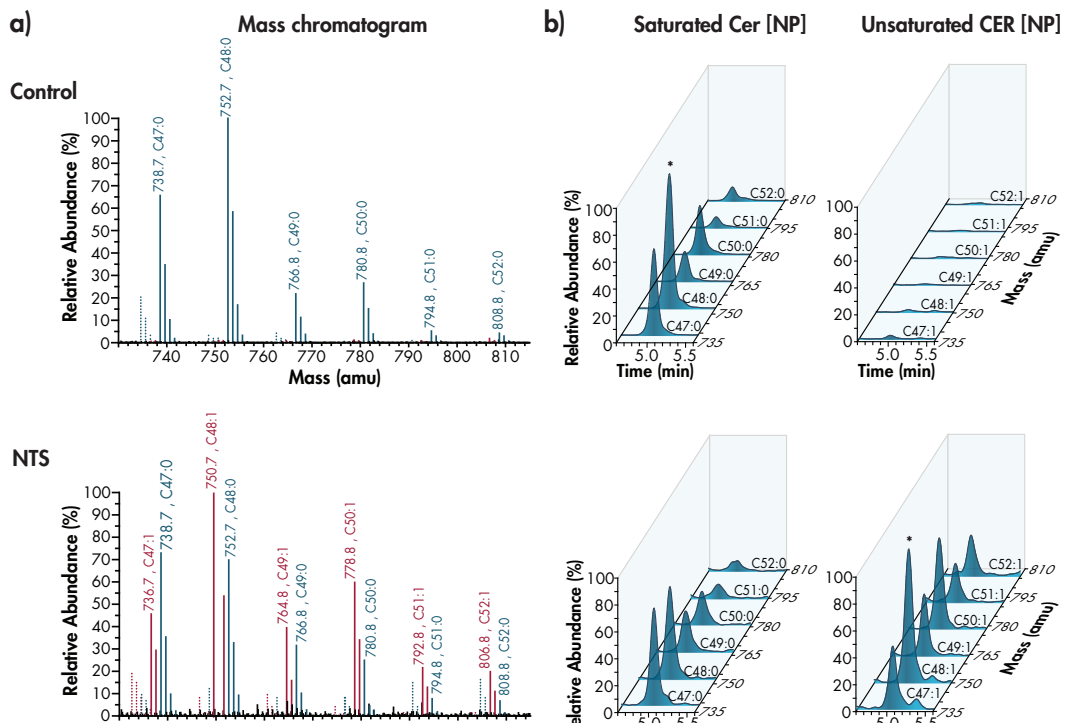

Figure 5: ***a****) Mass chromatograms of a subsection (730-815 amu) of CER [NP] in a representative control subject (upper chromatogram) and NTS patient (lower chromatogram). Peak labels indicate the mass (amu) and to which CER chain length and degree of unsaturation it corresponds. Red lines indicate the unsaturated CERs observed in NTS patients. Although $[M+H]^+$ was the main ion observed, also the $[M+H\text{-}H_2O]^+$ is detected and shown in the chromatograms as dotted lines. These have a mass that is 18 amu lower than their main $[M+H]^+$ counterpart. Figure* ***b****) shows the 3D ion chromatograms of Figure* ***a****). Saturated and unsaturated chromatograms are presented separately in the left and right column respectively. Chromatograms are normalized to their highest peak in the sample and marked by *: i.e. CER [NP] C48:0 in the control subject and CER [NP] C48:1 in NTS patient.*

length of about ≤38 carbon atoms), all NTS patients show an increase compared to control subjects (27.2 ± 6.0% and 8.5 ± 1.3%, respectively).

A closer examination of the mass spectra led to the observation of unidentified peaks present in many CER subclasses, with a mass of exactly 2 amu lower compared to the identified CERs. As an example, this is illustrated in the mass chromatogram of Figure 5a, in which a subsection of the mass spectrum of CER [NP] is shown. These peaks correspond to CERs with one degree of unsaturation. The increase in unsaturated CERs in NTS is high, and the example of CER [NP] is illustrated in Figure 5b: The 3D ion chromatograms show the same subsection of CER [NP] in a control sample and a NTS patient. No unsaturated CERs were observed in control subjects, and the most abundant peak in this subsection corresponded to a saturated CER with a chain length of 48 carbon atoms. On the contrary, multiple peaks corresponding to unsaturated CERs of different chain length were observed in the NTS patient. In this subsection of CER [NP], unsaturated C48:1 was the most abundant peak. When comparing all the lipid profiles, it becomes apparent that NTS subject ⑥ does show the highest abundance of unsaturated CERs.

Altered lamellar lipid organization in Netherton syndrome

Figure 6 shows diffraction patterns of controls and NTS patients. The positions of the peaks are indicative for the periodicity of the lipid lamellae: a shift to higher *q*-values in the figure is indicative for a shorter periodicity (*d*) of the lipid lamellae. Figure 6a shows diffraction patterns of control SC. In previous studies, the diffraction patterns were analyzed and attributed to the two lamellar phases with repeat distances of around 13 (LPP) and 6 nm (SPP). All controls show clear peaks at scattering vector values (*q*) of 1.00 ± 0.01 and 1.45 ± 0.01 nm^{-1}. The 1.00 nm^{-1} diffraction peak is attributed to the 2nd order peak of the LPP and the 1st order peak of the SPP, whereas the 1.45 nm^{-1} peak is attributed to the 3rd order of the LPP. In addition, some controls also show the 1st order of the LPP as a weak shoulder at a *q*-value located at ~0.50 nm^{-1}. Figures 6b and 6c show diffraction patterns of NTS patients. SAXD patterns of NTS patients (numbers ①,⑤,⑥,⑦, and ⑧), who clearly showed acyl-CERs present in their 3D ion chromatograms of Figure 3 and Supplement 1, are depicted in Figure 6b. The presence of a diffraction peak at 0.5 nm^{-1}, but also the presence of peak '2' and '3' in patients ①,⑤,⑦, and ⑧ suggests that the LPP is present. The diffraction pattern of patient ⑧ is very similar to that of the controls, although the peak position indicated by '2' is shifted to slightly higher *q*-values suggesting a reduction in the repeat distances of the lamellar phases. The other diffraction patterns show distinct differences. In the SAXD pattern of SC from patients ①, ⑤, and ⑦, the peak indicated as '3' has a higher intensity compared that that in the controls and shifted to

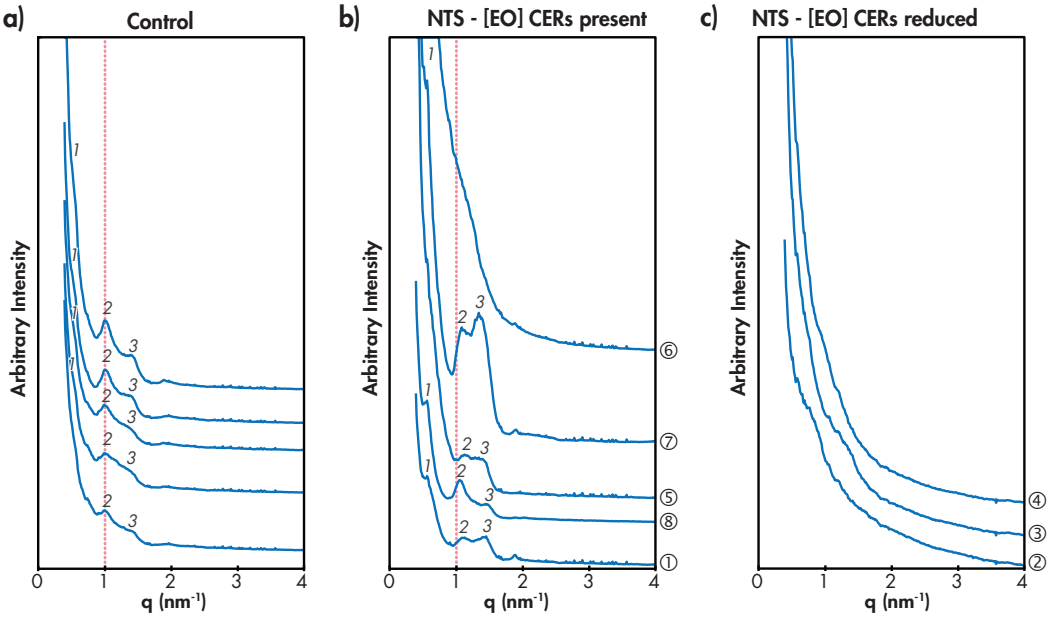

Figure 6: *SAXD patterns of controls **a**) and NTS patients (**b** and **c**). The positions of the peaks (q) are indicative for the periodicity of the lipid lamellae. Figure **b**) shows NTS patients with a normal level of acyl-CERs, while Figure **c**) presents diffraction patterns of NTS patients with a reduced level of acyl-CERs. From the scattering angle, the scattering vector (q) was calculated by $q = 4\pi \sin \theta/\lambda$, in which λ is the wavelength of the X-rays at the sample position and θ the scattering angle. Individual NTS patients are labeled ①-⑧.*

either lower or higher *q*-values. The most likely explanation for this increased intensity and changed shape of the peak is the formation of additional phases. The diffraction pattern of patient ⑥ does not show any diffraction peak. Figure 6c shows the SAXD curves of the NTS patients (numbers ②,③, and ④) that have a low level of acyl-CERs present in the 3D ion chromatograms in Figure 3. No peaks are observed in the diffraction patterns of these NTS patients.

Higher degree of disordering of the lipid chains in NTS

Figure 7 shows the CH_2 symmetric stretching peak position of the SC lipids in controls (green) and NTS patients (red). A higher peak position indicates a higher degree of conformational disordering of the lipid chains. The average peak position of the NTS patients is 2850.0 ± 0.6 cm^{-1}, which is significantly higher compared to the control samples, showing an average value of 2849.4 ± 0.1 cm^{-1}. In addition, a larger variability between NTS patients compared to controls was observed when performing a non-parametric Levene's test ($P<0.05$).

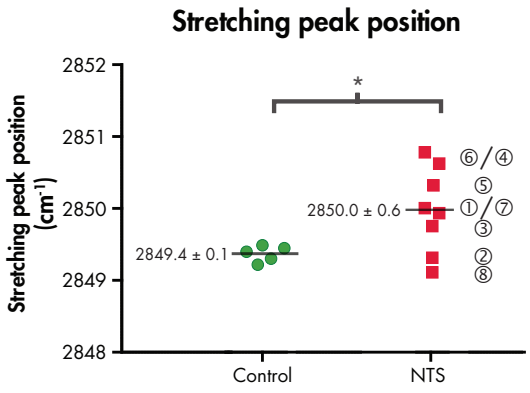

Figure 7: *CH_2 symmetric stretching peak position in SC of controls (green dots) and NTS patients (red dots). A higher peak position indicates a higher degree of conformational disordering of the lipid chains. Individual NTS patients are labeled ①-⑧.*

Discussion

In this study, we investigated the SC lipid composition and organization in 8 NTS patients and compared this to control SC. Recently, Bonnart *et al*. studied the lipid composition in transgenic mice overexpressing ELA2 as a model for NTS[34]. They observed a decreased level of FFAs and an increased total level of glucosylceramide and reduction of sphingomyelin. Electron microscopy studies revealed the presence of unprocessed lipids in the intercellular space of the SC. However, no further details on lipid subclasses and chain length distributions were provided, which is the focus of the present study. In addition we analyzed the lipid organization. Both the lipid composition and organization in SC of NTS patients show large deviations from that in control subjects. More precisely, we show that in SC of NTS patients there is an increase in the levels of MUFAs and in short-chain FFAs. Similar changes were observed in the CER composition: increased levels of unsaturated CERs as well as short-chain CERs were abundantly present in SC of NTS patients compared to control subjects. We also observed changes in the lipid organization in SC of NTS patients: a higher degree in conformational disordering of the lipid chains as well as an altered lamellar organization. In a subgroup of NTS patients almost no acyl-CERs were present.

The changes in the lipid composition correlated to changes in the lipid organization. NTS patients (①,⑤,⑦, and ⑧) with normal levels of acyl-CERs in their SC, revealed a diffraction pattern indicating the presence of the LPP. In contrast, NTS patients with low levels of acyl-CERs (②,③, and ④) did not show any proper SC lamellar organization, as no diffraction peaks were observed in the corresponding SAXD profile. The exception is NTS patient ⑥: Despite a high level of acyl CERs present in the SC, no peaks were detected in the

SAXD profile of this patient. However, this patient shows a clearly distinguishable profile in most CER subclasses and has the highest level of short chain CERs and unsaturated CERs. In addition, the highest level of MUFAs as well as the shortest average FFA chain length was observed in this patient. The abundant presence of shorter and unsaturated lipid chains enhances disordering of the lipid organization and may therefore explain the lack of regularly stacked lipid lamellae[49]. Finally, only one patient (⑧) showed a diffraction profile very similar to the controls. This patient exhibits the least deviation in SC lipid composition compared to the control subjects.

It has been reported that NTS patients show a drastic reduction in skin barrier function, as indicated by increased TEWL values[7-9]. As the lipids play a crucial role in the skin barrier function, an altered lipid composition and thus a change in lipid organization may contribute to the increased TEWL values in NTS patients: In previous studies using model lipid systems, we observed that both an absence of acyl-CERs as well as short chain FFAs results in an increased permeability[49,50]. Furthermore, very recently we also reported an excellent correlation between a reduction in chain length of CERs and an increase in TEWL in patients with AE, demonstrating that the lipids may play a role in the impaired skin barrier function[17].

NTS and AE are both inflammatory diseases with some genetic association. Patients with NTS show many symptoms comparable to AE patients[18,19]. Therefore, a comparison in lipid profiling between NTS and AE is also of interest. Several changes in lipid composition in NTS were also observed in SC of patients with AE, but in the latter less pronounced. These changes are: *i)* A reduction in the level of acyl-CERs; *ii)* Increased levels of CER [AS] and CER [NS] and a reduced level of CER [NP]; *iii)* Increased levels in C34 CERs; *iv)* A shift to shorter chain lengths in FFAs and CERs; *v)* Increased levels in MUFAs. In AE, these changes in lipid composition correlated very well with an increased TEWL[16,17,51]. Therefore, also in NTS these changes in lipid composition and organization may contribute to the impaired skin barrier. In AE we observed that changes in the SC lipids were more pronounced in lesional skin compared to non-lesional skin, which may indicate that either inflammation and/or the presence of surface bacteria may play a role in changes in the lipid composition.

Several changes in epidermal processing may contribute to a change in the lipid composition in NTS. i) An increased pH in SC of NTS patients, which may be caused by an ELA-2 hyperactivity and lower NMF levels. This may lead to alterations in SC CER subclass levels in NTS[33,36,52] as the activity of both sphingomyelinase and β-glucocerebrosidase are both highly dependent on the pH in their microenvironment. Furthermore, a pH increase induces high serine proteases activity that in turn degrades lipid processing enzymes[33]. Upregulation of KLK activity has also been reported to affect these enzymes[33]. As CER

[AS] and CER [NS] both have sphingomyelin as precursor, an imbalance in the activity of these enzymes may increase the relative levels of these ceramides. ii) Park *et al*. showed a downregulation of elongases 1, 4 and 6 (ELOVL1, 4 and 6) and a subsequent reduction in CER chain length in a murine atopic eczema model[53], demonstrating that these enzymes may be involved in the reduction of CER chain length in this model. In addition, it is known that ELOVL-4 knockout mice show a strong reduction in long chain FFAs, especially beyond C24; increased presence of unsaturated FFAs; and absence of acyl-CERs[54]. Therefore, the reduction in chain length of the lipids in SC of NTS patients may be related to a decreased activity of ELOVLs.

In conclusion, this study indicates for the first time that the SC lipid composition and organization are both altered in NTS patients. These alterations in SC lipids may at least partly explain the skin barrier dysfunction in NTS. It is of interest to study the activity of the abovementioned enzymes in NTS patients *in vivo* as the SC lipid barrier is likely impaired due to altered epidermal enzyme activities in NTS patients.

References

1 Bitoun E, Chavanas S, Irvine AD *et al.* Netherton syndrome: disease expression and spectrum of SPINK5 mutations in 21 families. *J Invest Dermatol* 2002; 118: 352-61.

2 Hausser I, Anton-Lamprecht I, Hartschuh W *et al.* Netherton's syndrome: ultrastructure of the active lesion under retinoid therapy. *Arch Dermatol Res* 1989; 281: 165-72.

3 Pruszkowski A, Bodemer C, Fraitag S *et al.* Neonatal and infantile erythrodermas: a retrospective study of 51 patients. *Arch Dermatol* 2000; 136: 875-80.

4 Smith DL, Smith JG, Wong SW *et al.* Netherton's syndrome: a syndrome of elevated IgE and characteristic skin and hair findings. *J Allergy Clin Immunol* 1995; 95: 116-23.

5 Sun JD, Linden KG. Netherton syndrome: a case report and review of the literature. Int J Dermatol 2006; 45: 693-7.

6 Greene SL, Muller SA. Netherton's syndrome. Report of a case and review of the literature. *J Am Acad Dermatol* 1985; 13: 329-37.

7 Fartasch M, Williams ML, Elias PM. Altered lamellar body secretion and stratum corneum membrane structure in Netherton syndrome: differentiation from other infantile erythrodermas and pathogenic implications. *Arch Dermatol* 1999; 135: 823-32.

8 Hachem JP, Wagberg F, Schmuth M *et al.* Serine protease activity and residual LEKTI expression determine phenotype in Netherton syndrome. *J Invest Dermatol* 2006; 126: 1609-21.

9 Moskowitz DG, Fowler AJ, Heyman MB *et al.* Pathophysiologic basis for growth failure in children with ichthyosis: an evaluation of cutaneous ultrastructure, epidermal permeability barrier function, and energy expenditure. *J Pediatr* 2004; 145: 82-92.

10 Masukawa Y, Narita H, Sato H *et al.* Comprehensive quantification of ceramide species in human stratum corneum. *J Lipid Res* 2009; 50: 1708-19.

11 van Smeden J, Hoppel L, van der Heijden R *et al.* LC/MS analysis of stratum corneum lipids: ceramide profiling and discovery. *J Lipid Res* 2011; 52: 1211-21.

12 Norlen L, Nicander I, Lundsjo A *et al.* A new HPLC-based method for the quantitative analysis of inner stratum corneum lipids with special reference to the free fatty acid fraction. *Arch Dermatol Res* 1998; 290: 508-16.

13 Ponec M, Gibbs S, Pilgram G *et al.* Barrier function in reconstructed epidermis and its resemblance to native human skin. *Skin Pharmacol Appl Skin Physiol* 2001; 14 Suppl 1: 63-71.

14 Madison KC, Swartzendruber DC, Wertz PW *et al.* Presence of intact intercellular lipid lamellae in the upper layers of the stratum corneum. *J Invest Dermatol* 1987; 88: 714-8.

15 Bouwstra JA, Gooris GS, van der Spek JA *et al.* Structural investigations of human stratum corneum by small-angle X-ray scattering. *J Invest Dermatol* 1991; 97: 1005-12.

16 Ishikawa J, Narita H, Kondo N *et al.* Changes in the ceramide profile of atopic dermatitis patients. *J Invest Dermatol* 2010; 130: 2511-4.

17 Janssens M, van Smeden J, Gooris GS *et al.* Increase in short-chain ceramides correlates with an altered lipid organization and decreased barrier function in atopic eczema patients. *J Lipid Res* 2012; 53: 2755-66.

18 Elias PM. Therapeutic Implications of a Barrier-based Pathogenesis of Atopic Dermatitis. *Ann Dermatol* 2010; 22: 245-54.

19 Krol A, Krafchik B. The differential diagnosis of atopic dermatitis in childhood. *Dermatol Ther* 2006; 19: 73-82.

20 Chavanas S, Bodemer C, Rochat A *et al.* Mutations in SPINK5, encoding a serine protease inhibitor, cause Netherton syndrome. *Nat Genet* 2000; 25: 141-2.

21 Simon M, Bernard D, Minondo AM *et al.* Persistence of both peripheral and non-peripheral corneodesmosomes in the upper stratum corneum of winter xerosis skin versus only peripheral in normal skin. *J Invest Dermatol* 2001; 116: 23-30.

22 Komatsu N, Saijoh K, Otsuki N *et al.* Proteolytic processing of human growth hormone by multiple tissue kallikreins and regulation by the serine protease inhibitor Kazal-Type5 (SPINK5) protein. *Clin Chim Acta* 2007; 377: 228-36.

23 Komatsu N, Saijoh K, Sidiropoulos M *et al.* Quantification of human tissue kallikreins in the stratum corneum: dependence on age and gender. *J Invest Dermatol* 2005; 125: 1182-9.

24 Komatsu N, Takata M, Otsuki N *et al.* Elevated stratum corneum hydrolytic activity in Netherton syndrome suggests an inhibitory regulation of desquamation by SPINK5-derived peptides. *J Invest Dermatol* 2002; 118: 436-43.

25 Borgono CA, Michael IP, Komatsu N *et al.* A potential role for multiple tissue kallikrein serine proteases in epidermal desquamation. *J Biol Chem* 2007; 282: 3640-52.

26 Egelrud T, Brattsand M, Kreutzmann P *et al.* hK5 and hK7, two serine proteinases abundant in human skin, are inhibited by LEKTI domain 6. *Br J Dermatol* 2005; 153: 1200-3.

27 Deraison C, Bonnart C, Lopez F *et al.* LEKTI fragments specifically inhibit KLK5, KLK7, and KLK14 and control desquamation through a pH-dependent interaction. *Mol Biol Cell* 2007; 18: 3607-19.

28 Stefansson K, Brattsand M, Roosterman D *et al.* Activation of proteinase-activated receptor-2 by human kallikrein-related peptidases. *J Invest Dermatol* 2008; 128: 18-25.

29 Briot A, Deraison C, Lacroix M *et al.* Kallikrein 5 induces atopic dermatitis-like lesions through PAR2-mediated thymic stromal lymphopoietin expression in Netherton syndrome. *J Exp Med* 2009; 206: 1135-47.

30 Brattsand M, Stefansson K, Lundh C *et al.* A proteolytic cascade of kallikreins in the stratum corneum. *J Invest Dermatol* 2005; 124: 198-203.

31 Hatano Y, Terashi H, Arakawa S *et al.* Interleukin-4 suppresses the enhancement of ceramide synthesis and cutaneous permeability barrier functions induced by tumor necrosis factor-alpha and interferon-gamma in human epidermis. *J Invest Dermatol* 2005; 124: 786-92.

32 Jung YJ, Jung M, Kim M *et al.* IL-1 alpha Stimulation Restores Epidermal Permeability and Antimicrobial Barriers Compromised by Topical Tacrolimus. *Journal of Investigative Dermatology* 2011; 131: 698-705.

33 Hachem JP, Man MQ, Crumrine D *et al.* Sustained serine proteases activity by prolonged increase in pH leads to degradation of lipid processing enzymes and profound alterations of barrier function and stratum corneum integrity. *J Invest Dermatol* 2005; 125: 510-20.

34 Bonnart C, Deraison C, Lacroix M *et al.* Elastase 2 is expressed in human and mouse epidermis and impairs skin barrier function in Netherton syndrome through filaggrin and lipid misprocessing. *J Clin Invest* 2010; 120: 871-82.

35 Rippke F, Schreiner V, Schwanitz HJ. The acidic milieu of the horny layer: new findings on the physiology and pathophysiology of skin pH. *Am J Clin Dermatol* 2002; 3: 261-72.

36 Mauro T, Elias PM, Feingold KR. SC pH: measurement, origins, and functions. *In "Skin Barrier". New York: Taylor & Francis.* 2006.

37 Emami N, Diamandis EP. Human kallikrein-related peptidase 14 (KLK14) is a new activator component of the KLK proteolytic cascade. Possible function in seminal plasma and skin. *J Biol Chem* 2008; 283: 3031-41.

38 Michael IP, Pampalakis G, Mikolajczyk SD *et al.* Human tissue kallikrein 5 is a member of a proteolytic cascade pathway involved in seminal clot liquefaction and potentially in prostate cancer progression. *J Biol Chem* 2006; 281: 12743-50.

39 Raghunath M, Tontsidou L, Oji V *et al.* SPINK5 and Netherton syndrome: novel mutations, demonstration of missing LEKTI, and differential expression of transglutaminases. *J Invest Dermatol* 2004; 123: 474-83.

40 Di WL, Hennekam RC, Callard RE *et al.* A heterozygous null mutation combined with the G1258A polymorphism of SPINK5 causes impaired LEKTI function and abnormal expression of skin barrier proteins. *Br J Dermatol* 2009; 161: 404-12.

41 Hitomi K. Transglutaminases in skin epidermis. *Eur J Dermatol* 2005; 15: 313-9.

42 Hausser I, Anton-Lamprecht I. Severe congenital generalized exfoliative erythroderma in newborns and infants: a possible sign of Netherton syndrome. *Pediatr Dermatol* 1996; 13: 183-99.

43 Schreiner V, Gooris GS, Pfeiffer S *et al.* Barrier characteristics of different human skin types investigated with X-ray diffraction, lipid analysis, and electron microscopy imaging. *J Invest Dermatol* 2000; 114: 654-60.

44 Tanojo H, BosvanGeest A, Bouwstra JA *et al.* In vitro human skin barrier perturbation by oleic acid: Thermal analysis and freeze fracture electron microscopy studies. *Thermochimica Acta* 1997; 293: 77-85.

45 International Union of Pure and Applied Chemistry. Commission on the Nomenclature of Organic Chemistry., Rigaudy J, Klesney SP *et al. Nomenclature of organic chemistry, 4th edn. Oxford ; New York: Pergamon Press.* 1979.

46 Motta S, Monti M, Sesana S *et al.* Ceramide composition of the psoriatic scale. *Biochim Biophys Acta* 1993; 1182: 147-51.

47 Bligh EG, Dyer WJ. A rapid method of total lipid extraction and purification. *Can J Biochem Physiol* 1959; 37: 911-7.

48 Bras W, Dolbnya IP, Detollenaere D *et al.* Recent experiments on a combined small-angle/wide-angle X-ray scattering beam line at the ESRF. *Journal of Applied Crystallography* 2003; 36: 791-4.

49 Groen D, Poole DS, Gooris GS *et al.* Is an orthorhombic lateral packing and a proper lamellar organization important for the skin barrier function? *Biochim Biophys Acta* 2011; 1808: 1529-37.

50 de Jager M, Groenink W, Bielsa i Guivernau R *et al.* A novel in vitro percutaneous penetration model: evaluation of barrier properties with p-aminobenzoic acid and two of its derivatives. *Pharm Res* 2006; 23: 951-60.

51 van Smeden J, Janssens M, Kaye EC *et al.* The essence of the lipid chain length for skin barrier function and its relation to atopic eczema. To be submitted.

52 Hachem JP, Crumrine D, Fluhr J *et al.* pH directly regulates epidermal permeability barrier homeostasis, and stratum corneum integrity/cohesion. *J Invest Dermatol* 2003; 121: 345-53.

53 Park YH, Jang WH, Seo JA *et al.* Decrease of ceramides with very long-chain fatty acids and downregulation of elongases in a murine atopic dermatitis model. *J Invest Dermatol* 2012; 132: 476-9.

54 Vasireddy V, Uchida Y, Salem N, Jr. *et al.* Loss of functional ELOVL4 depletes very long-chain fatty acids (> or =C28) and the unique omega-O-acylceramides in skin leading to neonatal death. *Hum Mol Genet* 2007; 16: 471-82.

Supplementary Figure

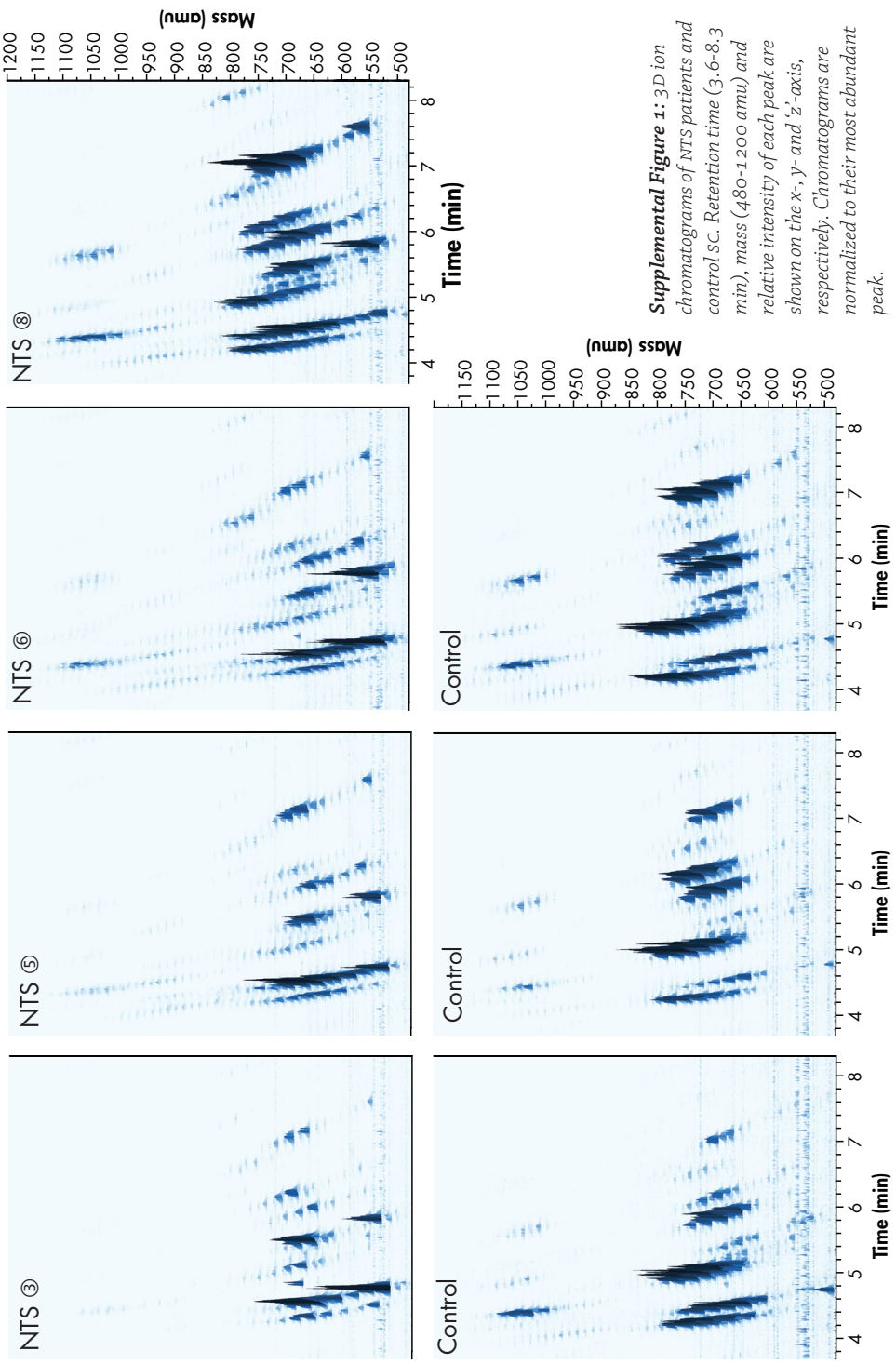

Supplemental Figure 1: *3D ion chromatograms of NTS patients and control SC. Retention time (3.6-8.3 min), mass (480-1200 amu) and relative intensity of each peak are shown on the x-, y- and 'z'-axis, respectively. Chromatograms are normalized to their most abundant peak.*